Received: September 2, 2021. Revised: October 22, 2021.

INASS

International Journal of
Intelligent Engineering & Systems

http://www.inass.org/

A Novel Improved VGSTA BS_SM Control Structure for Vector Control of High Performance SPIM Drives

Ngoc Thuy Pham[1]* **Thuan Duc Le[1]**

[1]*Dept. of Electrical Engineering Technology, Industrial University of Ho Chi Minh City*
* Corresponding author's Email: ngocpham1020@gmail.com

Abstract: In this paper, a new adaptive nonlinear control structure with VGSTA used to improve the performance and robustness of the BS and Sliding mode SM controllers for vector control of SPIM is proposed. In this proposal, the VGSTA algorithm is developed for BS_SM controller with the gains are updated continuously during the operation process, on the one hand, it provides precise, instantaneous output responses, on the other hand, enhances the robustness and stability of SPIM drive systems. The use the VGSTA for both outer-loop BS controller and inner-loop SM controller is an effective choice for the control of uncertain nonlinear systems since it overcomes the main drawbacks of the conventional BS_SM controller, that is, large control effort and chattering phenomenon. The obtained simulation results have confirmed that the speed, rotor flux and torque ripples are significantly minimized for entire speed range, the SPIM drives give fast and accurate dynamic responses under change in the machine parameters, load disturbances and different working conditions, especially, significantly chattering phenomenon alleviation. The obtained results by simulation using the Matlab tool verified the performances of the proposed control algorithm.

Keywords: Backstepping control, Sliding mode control, Variable gain super twisting algorithm, Six phase induction motor drives, FOC vector control.

1. Introduction

The SPIM drives are widely applied in many fields in industry, transportation, …etc. The object of this paper is for improvement and enhancement control quality of the SPIM drive system using modern control techniques, this research direction not only reduce costs but also enhance the quality and the robustness of drive systems [1, 2].

As we know, the PID controller with the fixed gains in traditional FOC control does not satisfy the requirements of the high performance SPIM drives [3]. Therefore, the modern nonlinear control strategies have been developed and received great attention such as linear feedback, sliding model SM, BS, Fuzzy Logic and neural network (NN), predictive control, etc. In the feedback linearizing technique proposed in [4] cancels the nonlinear terms in the machine model, it is designed to achieve input–output decoupling. However, the parametric deviation will significantly affect the dynamic performance and the stability for practical implementation. By contrast, the BS control [5, 6] doesn't cancel all the nonlinearity. This approach offers great flexibility in the synthesis of the regulator and pursues the objectives of stabilization and tracking. However, the information of detailed and accurate system dynamic was required in the traditional BS scheme, which is difficult to obtain in practical application. In another approach, the fuzzy logic controller is used to deal with the unknown nonlinear functions and uncertain parameters. This is because Fuzy logic controller does not require a mathematical model. It is capable of handling the non-linear systems and generates human logic linguistic rules [7]. However, the performance of this controller depends on its input and output membership functions. Neural networks (NN) also has been successfully used for the control of dynamic system and identification [8]. The high computation rate, learning, and adaption capability of NN makes them ideal for adaptive control systems. However,

using NN to enhance the performance of the controller will require the computational burden compare to the conventional controllers. Finally, one of the most common nonlinear control methods today is the sliding mode control. The success of SM control is mainly due to its disturbance rejection, strong robustness, fast response and simple implementation [9]. However, when designing the SM controller, the switching gain should be larger than uncertainties that are assumed to be bounded to ensure its robustness so the choice of an excessive switching gain causes the chattering phenomenon. This phenomenon has a negative impact on the actuators of the system and can deteriorate the controlled systems if the control has a physical sense [9].

From the above analysis, we see that these nonlinear control techniques are usually quite complex, demanding high computational effort, and requiring a precise mathematical model. They were difficult to obtain satisfactory control performance when using independently, especially in the cases applied to control the nonline systems. On the other hand, as we knew, the design of FOC vector control system for high-performance SPIM drives have to comply with the basic design principle of FOC vector control. Therefore, the choice and combination the nonlinear control methods to match the characteristics of the inner and outer loop control of the FOC method for SPIM drive have been researching and developing[10, 12-15]. In [10], the authors proposed a control structure combining BS and SOSM controller, in that, BS controller applied in the outer rotor flux and speed loop controller, SOSM controller is proposed for inner current loop control to improve the control quality and ensure the stability of the SPIM drives. However, besides the outstanding advantages presented, the BS_SOSM control structure also has some disadvantages such as the chattering phenomenon, dynamic response and stability, robustness of the system under the uncertain/disturbance. To overcome these disadvantages, the authors continue to improve the BS_SM control construct in [10] by using the improved VGSTA algorithm for both the SM inner current control loop controller and the BS outer speed control loop controller for FOC vector control of a SPIM drive. The novelty featured in this study are:

- The improved variable gain super twisting algorithm are developed for both BS and SM controllers of FOC vector control of SPIM drives. The variable gain approach is introduced in super twisting algorithm to compensate the disturbances whose gradients bound dependent on the states. If the gain is selected as a linear function of disturbance bounds, finite time robust convergence can be achieved and reduce the magnitude of chattering effect [16]. Besides, the gain updated in the VGSTA algorithm also help to compensate for the machine parameter variations and load disturbances. This algorithm has simple control laws and assures an improvement in sliding accuracy with respect to conventional sliding mode control, give very fast and exact dynamic responses under uncertain load subject to variations in inertia and system friction, guarantees the robustness and stability of the controlled system. It is an effective tool for the control of uncertain nonlinear systems since it overcomes the main drawbacks of conventional sliding mode control, that is, large control effort and chattering.

- The proposed improved controller structure developed for SPIM is reasonable and accordance with the requirements of each control loop in the SPIM's FOC vector control, so it enhances the control quality and performance as well as the robustness of drive systems.

The rest of the paper is organized as follows. Section II presents the mathematical model of SPIM, the controller design is explained in Section III. Simulation results are provided in Section IV. Section V draws some conclusions.

2. Model vector control of SPIM drives

2.1 Model vector control of SPIM drives

The system includes the six phase induction motor fed by a SPVSI and a DC link. A diagram of the SPIMD is illustrated as in Fig. 1. In this part, vector space decomposition technique also has applied as in [17], the original six-dimensional space of the machine is transformed into three two-dimensional orthogonal subspaces in the stationary reference frame (D-Q), (x - y) and (zl -z2). This transformation is obtained by means of 6 x 6 transformation matrix:

$$T_6 = \frac{1}{\sqrt{3}}\begin{bmatrix} 1 & -\frac{1}{2} & -\frac{1}{2} & \frac{\sqrt{3}}{2} & -\frac{\sqrt{3}}{2} & 0 \\ 0 & \frac{\sqrt{3}}{2} & -\frac{\sqrt{3}}{2} & \frac{1}{2} & \frac{1}{2} & -1 \\ 1 & -\frac{1}{2} & -\frac{1}{2} & -\frac{\sqrt{3}}{2} & \frac{\sqrt{3}}{2} & 0 \\ 0 & -\frac{\sqrt{3}}{2} & \frac{\sqrt{3}}{2} & \frac{1}{2} & \frac{1}{2} & -1 \\ 1 & 1 & 1 & 0 & 0 & 0 \\ 0 & 0 & 0 & 1 & 1 & 1 \end{bmatrix} \quad (1)$$

To build SPIM model, some basic assumptions should be made. First, the windings are seen as to be sinusoidal distribution, the mutual leakage

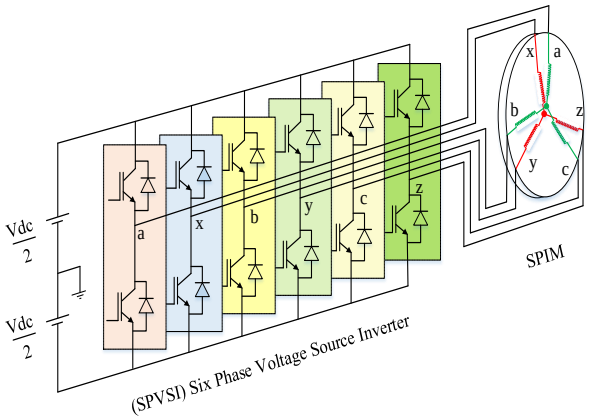

Figure. 1 A SPIM drive general diagram

inductances, the magnetic saturation, and the core losses are neglected. The math equations of SPIM be written in the stationary reference frame as

$$\begin{aligned}[V_s] &= [R_s][I_s] + p\{[L_s][I_s] + [L_m][I_r]\} \\ 0 &= [R_r][I_r] + p\{[L_r][I_r] + [L_m][I_s]\}\end{aligned} \quad (2)$$

The electromechanical energy conversion only takes place in the DQ subsystem. The torque equation can be written as follows:

$$T_e = 3P(\psi_{rQ} i_{rD} - \psi_{rD} i_{rQ}) \quad (3)$$

As we knew, (x-y) and (zl-z2) subspace produced losses, the electromechanical conversion just takes place in the D-Q subspace [1]. Therefore, the control is based on determining the applied voltage in the DQ reference coordinates. The SPIM control technique is similar to the three phase IM, the control for the motor in the stationary reference coordinates is difficult, even for a three phase IM, so the transformation of SPIM model in a dq rotating reference coordinates to obtain currents with dc components is necessary. A transformation matrix as in Eq. (4) be used.

$$T_{dq} = \begin{bmatrix} cos(\delta_r) & sin(\delta_r) \\ -sin(\delta_r) & cos(\delta_r) \end{bmatrix} \quad (4)$$

FOC is one of the most common control methods, Unlike the scalar control, FOC can improve the static and dynamic behavior of SPIM. FOC control can control torque and magnetic flux separately as the control way to DC motor. In that, the electromagnetic torque will be controlled by the i_{sq} stator current component, the rotor flux will be controlled by the i_{sd} stator current component. We have:ψ_{rq}= 0, ψ_{rd}= ψ_{rd}.

The new dynamics model of motor is described by the space vector differential equations:

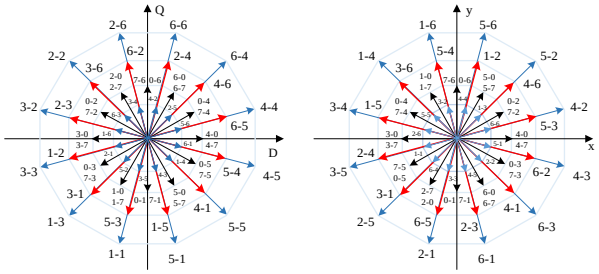

Figure. 2 Voltage space vectors and switching states in the (D-Q) and (x-y) subspaces for a SPVSI

$$\begin{cases} L_s \frac{di_{sd}}{dt} = -ai_{sd} + L_s\omega_e i_{sq} + bR_r\psi_{rd} + cu_{sd} \\ L_s \frac{di_{sq}}{dt} = -ai_{sq} + L_s\omega_e i_{sd} + b_r\omega_e\psi_{rd} + cu_{sq} \\ \frac{d\omega_r}{dt} = \frac{3}{2}P\frac{\delta\sigma L_s}{J}(\psi_{rd} i_{sq}) - \frac{T_l}{J} - B\omega_r \\ \frac{d\psi_{rd}}{dt} = \frac{L_m}{\tau_r} i_{sd} - \frac{1}{\tau_r}\psi_{rd} \end{cases} \quad (5)$$

where

$$\sigma = 1 - \frac{L_m^2}{L_s L_r}; \delta = \frac{L_m}{\sigma L_s L_r}; a = \frac{L_m^2 R_r + L_r^2 R_s}{\sigma L_r^2}; b = \frac{L_m^2 R_r}{\sigma L_r^2}; c = \frac{1}{\sigma} \quad (6)$$

The sliding frequency are expressed as follows:

$$\omega_{sl} = \frac{L_m}{L_r}\psi_r i_{sQ} \quad (7)$$

3. VGSTA BS_SM controller

3.1 The proposed VGSATBS controller for outer speed and rotor flux loops

In this part, an adaptive VGSTA_BS technique is proposed for vector control of SPIM drives. The stability and performance of the control systems is studied using the Lyapunov theory [17]. BS technique is a systematic and recursive method for synthesizing nonlinear control laws. So a virtual command, that will be generated to ensure the convergence of the systems to the equilibrium states. It allows the synthesis of robust control law despite different types of disturbances and parametric uncertainties. In this proposal, the robustness of this scheme is improved by introducing integral terms of the tracking errors in the control design. Beside this modified BS technique also is combined with VGSTA to increase its robustness under the parameter uncertainties and external load

disturbances and overcome the chattering problem of the classical sliding-mode techniques. The speed and rotor flux error tracking function defined:

$$\varepsilon_\omega = (\omega_r^* - \omega_r) + k_\omega \int_0^t (\omega_r^* - \omega_r)dt$$
$$\varepsilon_\psi = (\psi_{rd}^* - \psi_{rd}) + k_\psi \int_0^t (\psi_{rd}^* - \psi_{rd})dt \quad (8)$$

Differentiating ε and Combining formula (5), we get:

$$\dot{\varepsilon_\omega} = \dot{\omega^*} - \frac{3P}{2}\frac{\delta\sigma L_s}{J}\psi_{rd} i_{sq}^* + \frac{T_l}{J} + B\omega + k_\omega'(\omega^* - \omega)$$
$$\dot{\varepsilon_\psi} = \dot{\psi_{rd}^*} - \frac{L_m}{\tau_r} i_{sd}^* + \frac{1}{\tau_r}\psi_{rd} + k_\psi'(\psi_{rd}^* - \psi_{rd}) \quad (9)$$

To obtain the virtual controller of speed and rotor flux loop, the following Lyapunov function candidate is considered:

$$V_{(\omega,\psi)} = \frac{1}{2}(\varepsilon_\omega^2 + \varepsilon_\psi^2) \quad (10)$$

Differentiating *V* and Combining formula (5), we get:

$$\dot{V}_{(\omega,\psi)} = \varepsilon_\omega \dot{\varepsilon_\omega} + \varepsilon_\psi \dot{\varepsilon_\psi} = \varepsilon_\omega \left\{\dot{\omega_r}^* - \frac{3P}{2}\frac{\delta\sigma L_s}{J}\psi_{rd} i_{sq}^* + \frac{T_L}{J} + B\omega_r + k_\omega(\omega_r^* - \omega_r)\right\} + \varepsilon_{\psi_{rd}}\left\{\dot{\psi_{rd}^*} - \frac{L_m}{\tau_r} i_{sd}^* + \frac{1}{\tau_r}\psi_{rd} + k_\psi(\psi_{rd}^* - \psi_{rd})\right. \quad (11)$$

where k_ω, k_Ψ are positive constants. To $V' < 0$, the stabilizing virtual controls are chosen as

$$i_{sq}^* = \frac{1}{k_t\psi_{rd}}\left\{k_\omega\varepsilon_\omega + \dot{\omega^*} + B\omega + \frac{T_L}{J} + k_\omega'(\omega^* - \omega)\right\} + \Pi_\alpha$$

$$i_{sd}^* = \frac{\tau_r}{L_m}\left\{k_\psi\varepsilon_\psi + \dot{\psi_{rd}^*} + \frac{1}{\tau_r}\psi_{rd} + k_\psi'(\psi_{rd}^* - \psi_{rd})\right\} + \Pi_\beta \quad (12)$$

where, Π_α,Π_β are the control signals injected in order to improve the performance of BS controller.

The load torque T_L is estimated:

$$T_L = \frac{1}{1+\tau_0 p}\left[\left(\frac{3}{2}P\frac{L_m}{L_r}\psi_{rd} i_{sq}\right) - \frac{J}{P}\frac{d\omega_r}{dt}\right] \quad (13)$$

where: τ_0: is time gain;

The variable gain approach is introduced in super twisting algorithm in order to compensate disturbances whose gradients bounds are dependent on the state [16]. If the gain is selected as a linear function of disturbance bounds, finite time robust convergence can be achieved. An improved VGSTA developed has the form:

$$\Pi_\alpha = k_{\alpha\omega 1}(t, \varepsilon_{isd})\left[\delta_1\phi_{\omega 1}(S_1) + \mu_1\int_0^t \phi_{\omega 2}(S_1)dt\right]$$
$$\Pi_\beta = k_{\alpha\omega 2}(t, \varepsilon_{isq})\left[\delta_2\phi_{\omega 1}(S_2) + \mu_2\int_0^t \phi_{\omega 2}(S_2)dt\right] \quad (14)$$

where,

$$\begin{cases} k_{\alpha\omega 1}(t, \varepsilon_{\mathrm{isd}}) = S_1 sat(S_1); k_{\alpha\omega 2}(t, \varepsilon_{\mathrm{isq}}) = S_2 sat(S_2) \\ \phi_{\omega 1}(S_x) = |S_x|^{1/2} sat(S_x) + k_3 S_x \\ \phi_{\omega 2}(S_x) = \frac{1}{2}sat(S_x) + \frac{3}{2}k_3|S_x|^{1/2} sat(S_x) + k_3^2 S_x \end{cases} \quad (15)$$

From Eqs. (11), (12), (14), and (15), we obtain:

$$\frac{dV_{(\omega,\psi)}}{dt} = -k_\omega'\varepsilon_\omega^2 - k_\psi'\varepsilon_\psi^2 - \varepsilon_\omega\Pi_\alpha - \varepsilon_\beta\Pi_\beta < 0 \quad (16)$$

The virtual controls in (12) are chosen to satisfy the control objectives and also provide references for the next step of the VGSTA SM controller design.

3.2 SMC design with the variable-gain super-twisting algorithm for in the inner current loops

In this part, a high-order nonlinear sliding control algorithm based on Lyapunov stability theory using the VGSTA is proposed for the inner current loops to increase robustness of overall system, minimizing the effects of parameter variations and unforeseen disturbances in the control process. The current error tracking function defined:

$$\varepsilon_{isd} = i_{sd}^* - i_{sd}; \qquad \varepsilon_{isq} = i_{sq}^* - i_{sq} \quad (17)$$

The corresponding nonlinear slip surface according to the current components is defined as follows:

$$\begin{cases} S_1 = \varepsilon_{\mathrm{isd}} + k_1|\int \varepsilon_{\mathrm{isd}}dt|^{1/2} sat(\int \varepsilon_{\mathrm{isd}}dt) \\ S_2 = \varepsilon_{\mathrm{isq}} + k_2\left|\int \varepsilon_{\mathrm{isq}}dt\right|^{1/2} sat\left(\int \varepsilon_{\mathrm{isq}}dt\right) \end{cases} \quad (18)$$

Combining formula (5), taking the time differential on both sides of Eq. (18), we get:

$$\begin{aligned}\frac{dS_1}{dt} &= \frac{d\varepsilon_{isd}}{dt} + \frac{d}{dt}\left[k_1\left|\int \varepsilon_{isd}dt\right|^{\frac{1}{2}} sat(\int \varepsilon_{isd}dt)\right] \\ &= \frac{di_{sd}^*}{dt} - \frac{1}{L_s}\left[-ai_{sd} + L_s\omega_e i_{sq} + bR_r\psi_{rd} + cu_{sd}\right] \\ &\quad + \frac{d}{dt}\left[k_1\left|\int \varepsilon_{isd}dt\right|^{\frac{1}{2}} sat(\int \varepsilon_{isd}dt)\right] = -v_1 \\ \frac{dS_2}{dt} &= \frac{d\varepsilon_{isq}}{dt} + \frac{d}{dt}\left[k_2\left|\int \varepsilon_{isq}dt\right|^{1/2} sat\left(\int \varepsilon_{isq}dt\right)\right] \\ &= \frac{di_{sq}^*}{dt} - \frac{1}{L_s}\left[-\mathrm{ai_{sq}} - \mathrm{L_s}\omega_e i_{\mathrm{sd}} - \mathrm{b}_r\omega_e\psi_{\mathrm{rd}} + \mathrm{cu_{sq}}\right] \\ &\quad + \frac{d}{dt}\left[k_2\left|\int \varepsilon_{\mathrm{isq}}dt\right|^{1/2} sat\left(\int \varepsilon_{\mathrm{isq}}dt\right)\right] = -v_2\end{aligned} \tag{19}$$

In this proposed we select the v_1, v_2 switching control functions:

$$\begin{cases} v_1(t) = k_{\alpha 1}(t, \varepsilon_{\mathrm{isd}})\left[\delta_1\phi_1(S_1) + \mu_1\int_0^t \phi_2(S_1)dt\right] \\ v_2(t) = k_{\alpha 2}\left(t, \varepsilon_{\mathrm{isq}}\right)\left[\delta_2\phi_1(S_2) + \mu_2\int_0^t \phi_2(S_2)dt\right] \end{cases} \tag{20}$$

where:

$$\begin{cases} \{k_{\alpha 1}(t, \varepsilon_{\mathrm{isd}}) = S_1 sat(S_1)\,; k_{\alpha 2}\left(t, \varepsilon_{\mathrm{isq}}\right) = S_2 sat(S_2) \\ \phi_1(S_x) = |S_x|^{1/2} sat(S_x) + k_3 S_x \\ \phi_2(S_x) = \frac{1}{2} sat(S_x) + \frac{3}{2}k_3|S_x|^{1/2} sat(S_x) + k_3^2 S_x \end{cases} \tag{21}$$

with x = 1:2, k1, k2, k3,δ1,δ2,μ1,μ2 are positive coefficients. From Equation (19) the virtual control functions of the current control loop are determined as follows:

$$\begin{aligned} u_{sd}^* &= \frac{L_s}{c}\left\{v_1(t) + \frac{di_{sd}^*}{dt} + \frac{d}{dt}\left[k_1\left|\int \varepsilon_{isd}dt\right|^{\frac{1}{2}} sat\left(\int \varepsilon_{isd}dt\right)\right]\right\} + \frac{1}{c}\left[ai_{sd} - L_s\omega_e i_{sq} - b_r R_r\psi_{rd}\right] \\ u_{sq}^* &= \frac{L_s}{c}\left\{v_2(t) + \frac{di_{sq}^*}{dt} + \frac{d}{dt}\left[k_1\left|\int \varepsilon_{isd}dt\right|^{\frac{1}{2}} sat\left(\int \varepsilon_{isq}dt\right) + \frac{1}{c}\left[ai_{sq} + L_s\omega_e i_{sd} + b_r\omega_e\psi_{rd}\right]\right.\right. \end{aligned} \tag{22}$$

We select the Lyapunov function:

$$V = \frac{1}{2}(S_1^2 + S_2^2) \tag{23}$$

Differentiate both sides of Eq. (23), combine with formulas (19) and (20) to get:

$$\begin{aligned} \frac{dV}{dt} &= -k_{\alpha 1}(t, \varepsilon_{\mathrm{isd}})S_1\left[\phi_1(S_1) + \int_0^t \phi_2(S_1)dt\right] \\ &\quad -k_{\alpha 2}\left(t, \varepsilon_{\mathrm{isq}}\right)S_2\left[\phi_1(S_2) + \int_0^t \phi_2(S_2)dt\right] \end{aligned} \tag{24}$$

From Eq. (24), we see that the differential of the Lyapunov function is always negative. Therefore the system is always stable.

4. Simulink and discussion

The performance of the proposed VGSTA BS_SM controller for FOC vector control of SPIM drive system is validated though simulation by using MATLAB software. In order to increase reliability, a comparison framework is establish, the similar surveys also are implemented for the BS_SOSM controller and with the other latest methods in [5, 10-13, 18], to confirm the effectiveness of the proposed algorithm. The analysis results also show the characteristic robustness of the proposed controller to uncertainty of machine parameter, external load disturbance, faster and more accurate dynamic response. The block diagram of system is shown in Fig. 3.

SPIM parameters: 220V, 50 Hz, 4 pole, 1450 rpm. Rs = 10.1Ω, Rr = 9.8546Ω, Ls = 0.833457 H, Lr = 0.830811 H, m = 0.783106H, Ji = 0.0088 kg.m2. Rr, Rs is nominal value of rotor and stator resistance.

4.1 The performance of SPIM under the load disturbance

This test is conducted to confirm the performance and robustness of the SPIM drive system under the load disturbance. In order to easily establish a comparison framework the proposed controller with others, this test is implemented based on recommended benchmark test in [11]. The reference speed is keep constant at 150 Rad/s, the sudden rated load is supplied at t = 0.5 s. The speed, torque, current, rotor flux responses of SPIM drive are shown in Fig.4. A similar survey also is implemented for the BS_SOSM controller to create comparison data (Table 1).

Comparing the survey results of the VGSTA BS_SM controller and BS_SOSM in Fig. 4 and the different controllers proposed in [Fig. 9d to 13d, 11], [Fig. 3, to Fig. 4, 5], [Fig. 6, 12], [Fig.10 to Fig. 17, 18] show that all proposed controllers give the speed, rotor flux, torque and stator current responses quite well. The speed, torque and rotor flux responses are fast and follow exactly the reference values. The speed deceleration occurs when applying the load but

fast stabilizing and converging to the reference values. However, it is easy to see that the VGSTABS_SM controller give the faster and more accurate speed response. Especially when facing to load disturbance, VGSTA BS_SM controller shown better controllability, works more stably and reliably.

Indeed, when observing the responses of the SMC-AW controller proposed in [Fig. 6, 12], we see occur overshoot when starting up 2.6 rad/s (~1.7%), the stabilizing and converging time to the reference values is 0.2 s, the speed deceleration occurs when applying the load is 7.5 rad/s (~ 4.7 %). The stabilizing and converging time to the reference values is 0.15s. BS_SOSM controller [10] and SVM-DTC-IOFL based on STSC controller [11] give better than the controller proposed in [12], the overshoot is not record, the stabilizing and converging time to the reference values is 0.125s and 0.11s, the speed deceleration occurs when applying the load is 0.9 rad/s and 0.65 rad/s, the stabilizing and converging time to the reference values is 0.012 s and 0.052 s, respectively. It is very important that the ability to control the speed from being affected by chattering is not reported in [12] while this is quite an important influence on the control quality of drive systems.

To further clarify the efficiency of this proposed controller, we continue to compare with the BS controller in [5] and DTC vector control in [18], the speed deceleration occurs when applying the load are 2.3 rad/s (~ 1.28 %) in [18] and 0.75 rad/s (~0.03%) in [5], the stabilizing and converging time to the reference values are 0.12s in [18] and 0.11s in [5], and the obtained simulation results in [5, 18] also shown that BS controller proposed in [5] and SVM_DTC vector control proposed in [18] give the torque, current and rotor flux ripples are quite large (Torque ripples are (~85%) in [5] and (~25%) in [18])). On the contrary, observing the Fig. 4 responses of VGSTA BS_SM, we see that the torque, current and rotor flux are better controlled, the error of tracking the reference speed in steady-state mode, overshoot in startup is almost zero, the speed deceleration occurs when applying the load is 0.6 rad/s (~0.4%), the stabilizing and converging time to the reference values is 0.051s. Especially, the Fig. 4 also show clear that the variable gain super-twisting with the adaptive characteristic of its gains help to eliminate the undesired chattering phenomenon, the ripple and overshoot of the torque and isdq current are significantly minimized for the entire survey process (Torque ripples are (~3.5%)).

Table 1. The comparative results of the robustness of SPIM drive at high speed range when using two different control when faced with the load disturbance

	BS_SOSM	VGSTA BS_SM
Dynamics	Good	Excellent
Accurate tracking	Good	Excellent
Stability properties	Good	Excellent
Robustness under load disturbance	Medium	Excellent
Chattering alleviation	Medium	Excellent

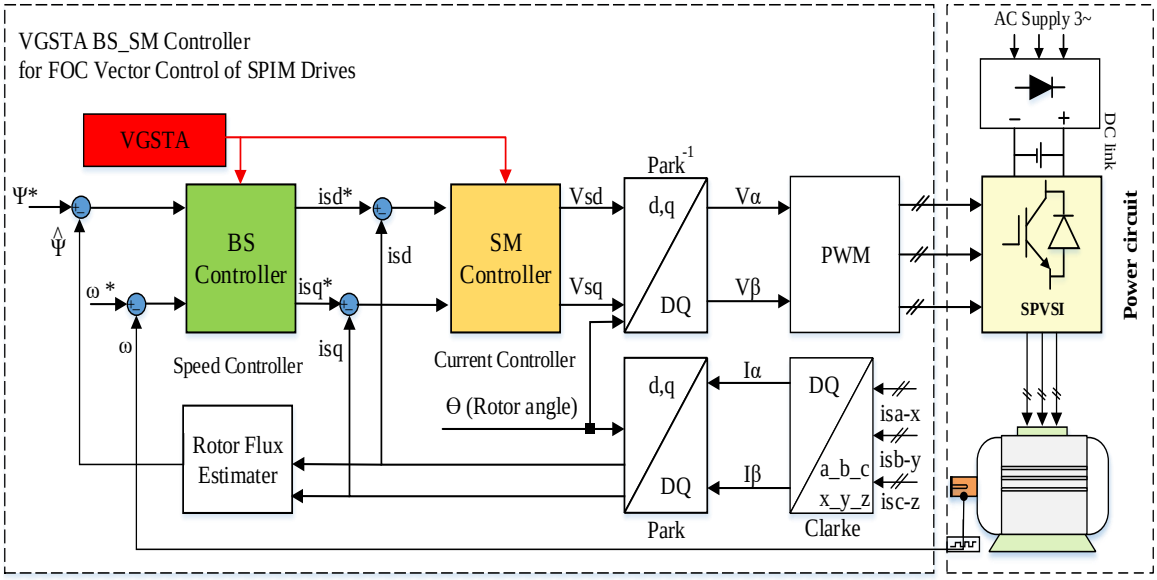

Figure. 3 FOC Vector control of SPIM drive using the novel improved VGSTA BS_SM control structure

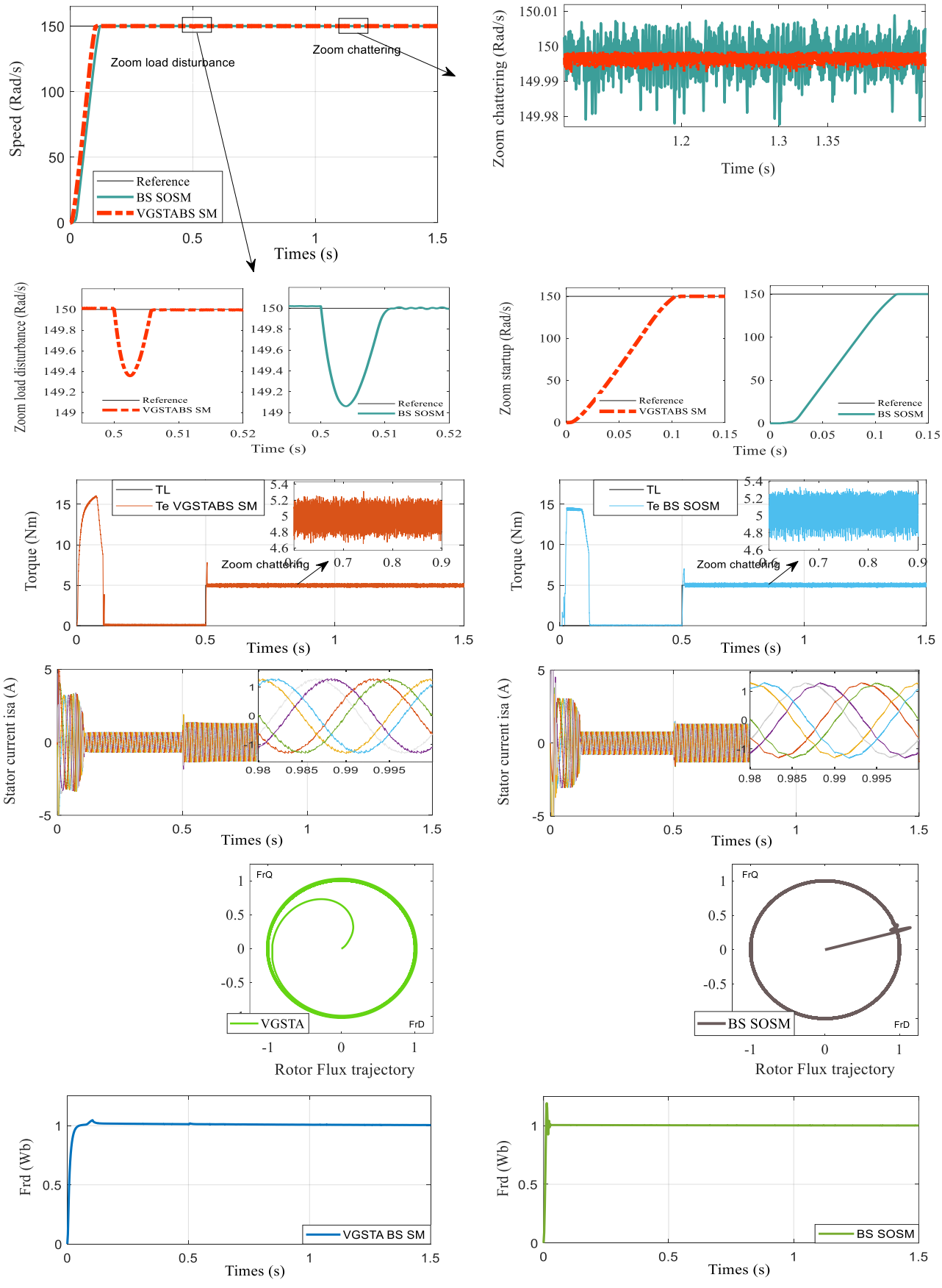

(a) (b)

Figure. 4 The performance of SPIM under the load torque disturbance: (a) VGSTABS_SM controller and (b) BS_SOSM controller

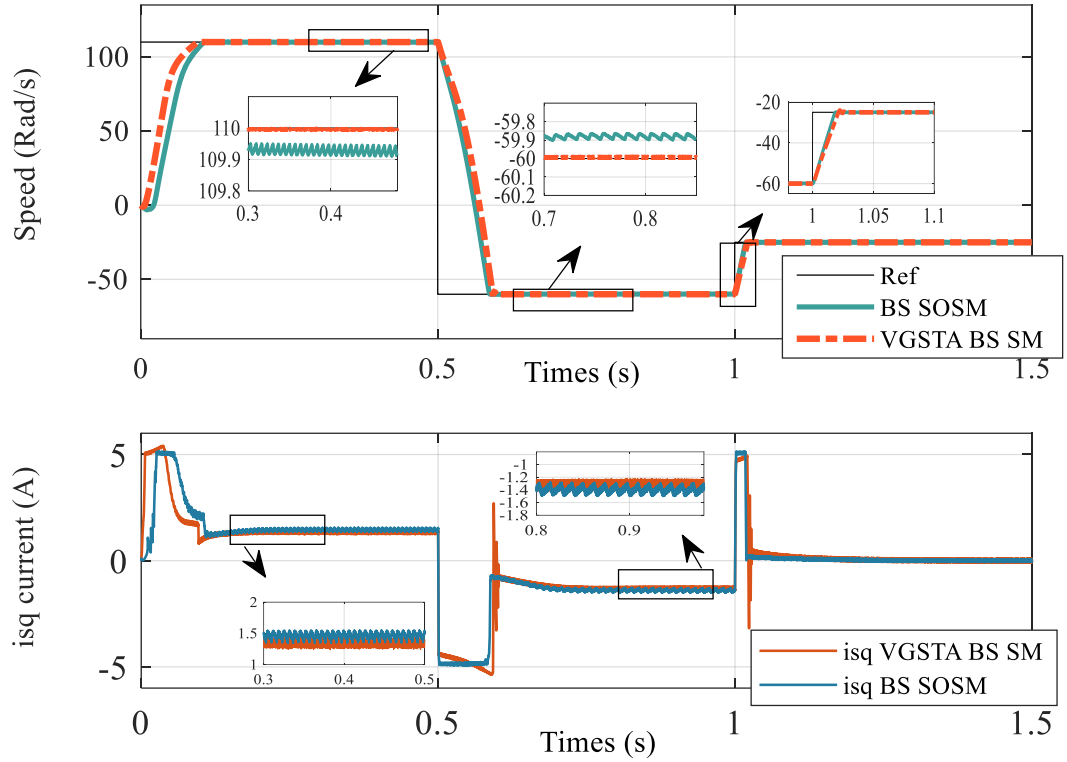

Figure. 5 The performance and robustness of the SPIM in case the speed, torque and Rr variations

Table 2. The comparative results the dynamic performance of SPIM on speed reversal when using two different control schemes with $R_r^* = 2\ R_r$

	BS_SOSM	VGSTABS_SM
Dynamics	Excellent	Excellent
Accurate tracking	Good	Excellent
Stability properties	Good	Excellent
Robustness under Rr variations	Good	Excellent

4.2 The dynamic performance of SPIM under the speed, torque and Rr variations

As we know that the τ_r rotor time constant has a great influence on the performance of the motor drive system in both the steady and transient working state. In fact, under the influence of heat, the R_r rotor resistance can increase twice times than its nominal value, hence, the speed error that caused τ_r is significantly.

In this test, the influence of R_r parametric variations to the robustness and stability of the SPIM drive system is considered, test is conducted based on recommended benchmark test in [Fig.5, 12]. In this survey, the reference speed is imposed from zero increased to 110, then decreased to −60 and then increased to −25 RPM, R_r rotor resistance is increased twice times its nominal value from at the beginning of the survey process. A similar survey also is implemented for the BS_SOSM controller, in order to establish a comparison framework. From simulink result in Figs. 5 and 6, we saw that the proposed VGSTABS_SM controller gives faster and more accurate responses than the BS_SOSM controller in [10] for all the surveyed speed steps. For the VGSTABS_SM controller, the real speed of motor is accurately tracking the reference speed, the speed error is almost zero. In contrast, with the BS_SOSM controller, the error between the actual speed of the motor exists (~1% rad/s). In particular, the Variable-Gain-Super-Twisting algorithm in VGSTABS_SM controller help significantly to improve the chattering phenomenon as showed in Figs. 5 and 6. Chattering is almost non-existent. In contrast, with the BS_SOSM controller, chattering occurs in both the high and low speed ranges, and in both forward rotation and reverse (Table. 2).

These simulink results also are compared with the obtained results with the ISMC-AW algorithm proposed in [12], it is easy to see that when working under Rr variation, the VGSTABS_SM controller give the better response, lower overshoot, faster

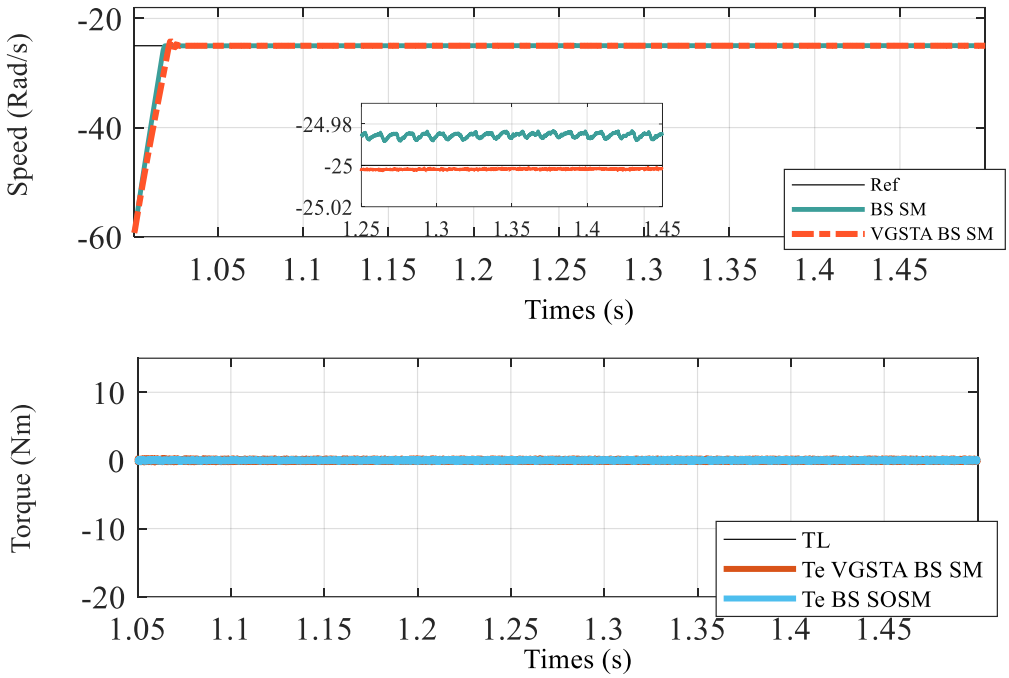

Figure. 6 The low speed under Rr variation ($R_r^* = 2\ R_r$), no load torque

Table 3. The comparative results between two different control schemes at low speed ranges at no load with $R_r^* = 2\ R_r$

	BS_SOSM	VGSTABS_SM
Dynamics	Excellent	Excellent
Accurate tracking	Good	Excellent
Stability properties	Good	Excellent
Robustness under Rr variations	Good	Excellent
Chattering alleviation	Medium	Excellent

dynamic responses significant than ISMC-AW algorithm. The chattering is not reported in detail in [12]. To more clarify the effectiveness of the proposed control algorithm, the comparison is made with the SM_PIAW Hybrid controller in [Fig. 11 and 13], the simulink results show that, the current controller of the VGSTA_SM control the i_{sq} current component better than the proposed current controller in [13]. During survey process, the phenomenon of i_{sq} current decreasing does not occur in both the steady and transient working state as in [Fig. 11 and 13], the i_{sq} current component in this proposed is equal as to the nominal R_r case.

Another survey also carried out to confirm robustness of SPIM under R_s, R_r Variations at low speed ranges. This test is conducted based on recommended benchmark test in [Fig. 19-20, 11]. In this test, the speed is keep by constant at 5% rated speed, external load step changes of 0 to 75% rated load at 0.5s, however, R_s and R_r are increased 100% at 1s ($R_r^*=2R_r$, $R_s^* =2R_s$) instead of R_r was keep constant by with normal rotor resistance value, only changed R_s stator resistance value increase 50% ($R_s^* =1.5R_s$, $R_r^*=R_r$) as in [11]. Fig. 7 shows the speed, torque responses of SPIM. Comparing these obtain results in Fig. 7 and the results in [Fig. 19b, 20b, and 11] show that three schemes have capability of handling low speed operation and large load changes are quite well. However, the performance and robustness of VGSTA BS_SM controller is the best in both the transient and steady state and when facing to load disturbance and R_s, R_r variation ($R_r^*=2R_r$, $R_s^* =2R_s$). Even working at low speed, sudden change of R_r rotor resistance variation does not affect to the performance and robustness of VGSTA BS_SM controller. The speed and torque response (Fig. 7a) are very well, the speed is keep constant and exactly by reference speed in almost the whole time of the survey, the chattering is almost eliminated. In contrast, with the BS_SOSM controller, error tracking before applying load is 0.018 (rad/s), when occurring R_r variation is 0.2 (rad/s). The chattering occurs in whole survey time, especially, chattering increase higher when R_r increases (Fig. 7b). These simulation results in Fig. 7 also shown that, even being surveyed under more extreme surveying condition but VGSTABS_SM controller gives better speed and torque response than the SVM-DTC-IOFL

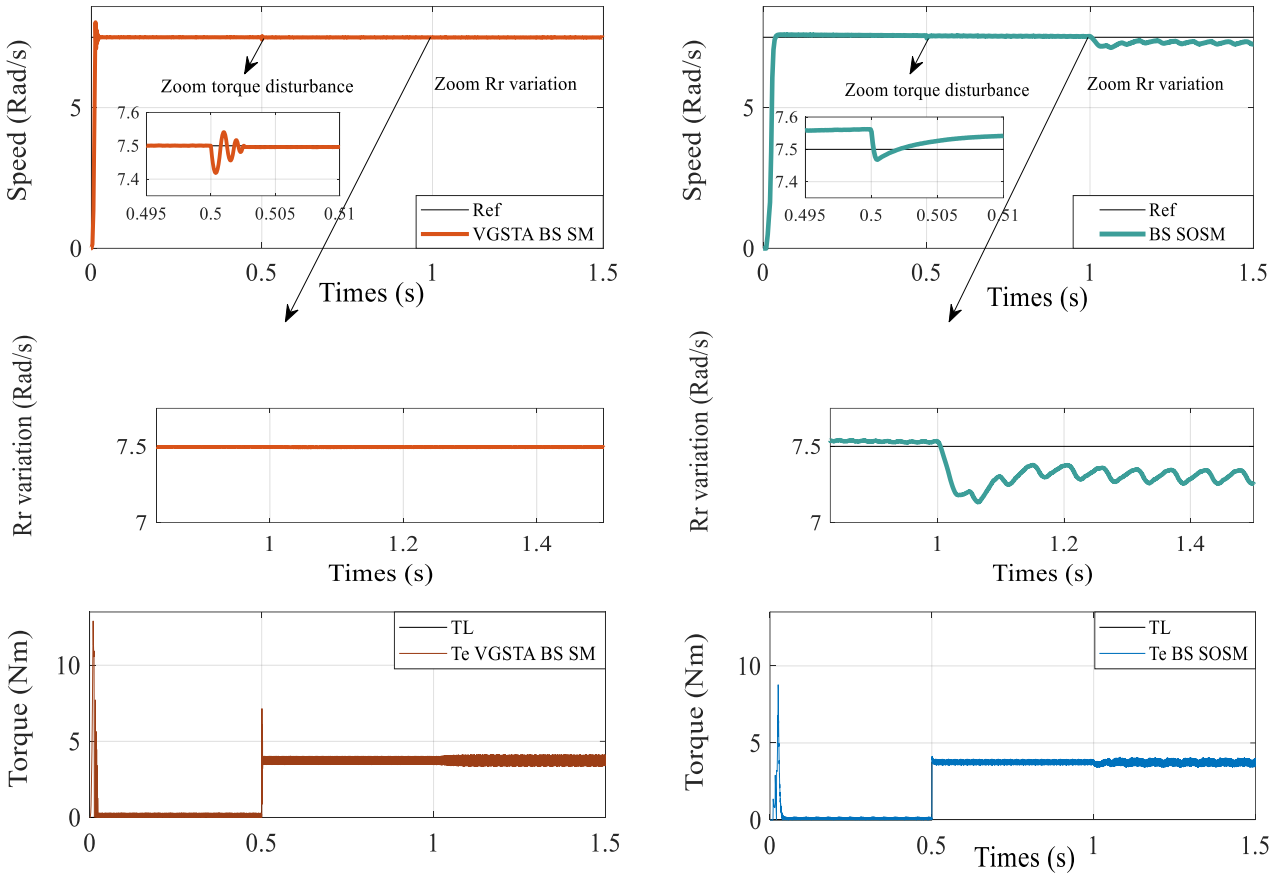

Figure. 7 The low speed (5% rated speed) under Rs, Rr and Torque variations (R*r=2Rr, R*s=2Rs at 1s; TL=75% rated load: (a) VGSTA BS_SM controller and (b) BS_SOSM controller

Table 4. The comparative results between two different control schemes at low speed ranges with 75% rated load under R*r=2Rr, R*s=2Rs

	BS_SOSM	VGSTABS_SM
Dynamics	Good	Excellent
Accurate tracking	Good	Excellent
Stability	Medium	Excellent
Robustness under load disturbance	Medium	Excellent
Robustness under Rr variations	Medium	Excellent
Chattering alleviation	Medium	Excellent

controller in [11] that surveyed in less harsh condition (Rr was keep constant by with normal rotor resistance value, only changed Rs stator resistance value increase 50% (Rs* =1.5Rs, Rr*=Rr). Through this survey we see that, the SVM-DTC-IOFL based on STSC in [11] gives a very good response in the high speed range [Fig. 9 to 13d, and 11], however, in the low speed range, under the condition of the extend load disturbance and machine parameter variations, the SVM-DTC-IOFL based on STSC gives the unsatisfactory responses for a high quality drive system.

From the simulation results, it is easy to see that the VGSTABS_SM proposed controller offers the best performance and robustness and the chattering phenomena elimination in all mention algorithms in this part. The obtained results are quite convincing since an improved nonlinear control construction using the variable gain super-twisting for BS_SM controller has significantly rejected the uncertainties and disturbances and the adaptive characteristic of its gains also help to the control effort effectively.

5. Conclusion

In this paper, a new nonlinear hybrid techniques VGSTA BS_SM is applied for the FOC vector control of SPIM drives. Through the survey process

in part 4, we saw that, although the proposed VGSTA algorithm for BS_SM requires less computation time than the control algorithm used in [5,9–12,18], it offers better performance and quality control. The gain updated in the VGSTA algorithm help to compensate for the machine parameter variations and load disturbances. This ensures the robustness of the drive systems. Further, the stability of the overall system also always ensured by Lyapunov stability criterion in entire design process. The use the VGSTA for both inner and outer loop control controller is an effective choice for the control of uncertain nonlinear systems since it inherits the robust and stable properties of BS_SOSM, overcomes the main drawbacks of the BS_SOSM controller, that is, large control effort and chattering. The obtained simulation results have confirmed that the speed, torque, current and rotor flux are better controlled, the error of tracking the reference speed in steady-state mode, overshoot in startup is almost zero, the speed deceleration occurs when applying the rated load is ~0.4%, the stabilizing and converging time to the reference values is 0.051s. The ripple of the speed, torque are significantly minimized in the entire survey process (Speed and torque ripples are 0.0001% and ~3.5%, respectively). Therefore, limiting problems arising during SPIM operation such as aging, mechanical vibrations, heating…etc. In the future, our group will continue to research and develop the hardware to address the experimental validation of VGSTA BS_SM controller.

Nomenclatures

VGSTA Variable Gain Super Twisting Algorithm
IM Induction Motor.
SPIM Six phase induction motor
BS Backstepping
SM Sliding Mode
SOSM Second Order Sliding Mode
SPVSI: Six Phase Voltage Source Inverter
FOC : Field Oriented Control.
ISMC-AW Integral Sliding Mode - Anti-Windup
DTC: Direct Torque Control
SVM: Space Vector Modulation
IOFL: Input-Output Feedback Linearization
PIAW Proportional Integral regulator Anti-Windup
V, I, ψ voltage, current, flux vector components
R, L, L_m Resistance, inductance, mutual inductance
δr rotor angular position referred to the stator
D-Q, x-y, z1-z2 Stationary reference frame
d-q Synchronous reference frame
*s,r,** Indices relating to stator, rotor, reference values
J, B Inertia moment, friction coefficient.
P Number of pole pairs
p Differential operator
T_e, T_L Electromagnetic torque and load torque.
$\omega_r, \omega_{sl}, \omega_e$ Rotor, slip angular, synchronous velocity.
τ_r, τ_s Rotor and stator time constant

Acknowledgments

This work was supported by the Industrial University of Ho Chi Minh City under Grant No. 112007003.

References

[1] E. Levi, “Multiphase electric machines for variable-speed applications”, *IEEE Trans. Ind. Electron.*, Vol. 55, No. 5, pp. 1893-1909, 2008.

[2] A.Oumar, R. Chakib, M. Labbadi, M. Cherkaoui, “Robust Nonlinear Controller of the Speed for Double Star Induction Machine in the Presence of a Sensor Fault”, *International Journal of Intelligent Engineering and Systems*, Vol. 13, No. 3, pp. 28-40, 2020.

[3] J. W. Finch and D. Giaouris, “Controlled AC electrical drives”, *IEEE Trans. Ind. Electron.*, Vol. 55, No. 2, pp. 481-491, 2008.

[4] F. Alonge, M. Cirrincione, M. Pucci, and A. Sferlazza, “Input–Output Feedback Linearization Control With On-Line MRAS-Based Inductor Resistance Estimation of Linear Induction Motors Including the Dynamic End Effects”, *IEEE Trans. Ind. Applications.*, Vol. 52, No. 1, pp. 254-266, 2016.

[5] H. Chaabaneo, K. D. Eddine, and C. Salim, “Sensorless backstepping control using a Luenberger observer for double-star induction motor”, *Archives of Electrical Engineering*, Vol. 69, No. 1, pp. 101-116, 2020.

[6] A. Zaafouri, C. B. Regaya, H. B. Azza, and A. Châari, “zDSP-based adaptive backstepping using the tracking errors for high-performance sensorless speed control of induction motor drive”, *ISA Transactions*, Vol. 60, pp. 333-347, 2016.

[7] H. Rahali1, S. Zeghlache, and L. Benalia, “Adaptive Field-Oriented Control Using Supervisory Type-2 Fuzzy Control for Dual Star Induction Machine”, *International Journal of Intelligent Engineering and Systems*, Vol. 10, No. 4, pp. 28-40, 2017.

[8] S. V. B. S. Reddy, B. Kumar, and D. Swaroop, “Investigations on Training Algorithms for Neural Networks Based Flux Estimator Used in Speed Estimation of Induction Motor”, In: *Proc. of 2019 6th International Conference on Signal*

Processing and Integrated Networks, pp. 1090-1094, 2019.

[9] R. Moutchou, A. Abbou, and S. E. Rhaili, "Super-Twisting Second-Order Sliding Mode Control of a Wind Turbine Coupled to a Permanent Magnet Synchronous Generator", *International Journal of Intelligent Engineering and Systems*, Vol. 14, No. 1, pp. 484-495, 2021.

[10] N. T. Pham, "Speed Tracking of Field Oriented Control SPIM Drive Using (BS_SOSM) Nonlinear control Structure", *WSEAS Transactions on Systems and Control*, Vol. 14, pp. 291-299, 2019.

[11] S. Krim, S. Gdaim, and M. F. Mimouni, "Robust Direct Torque Control with Super Twisting Sliding Mode Control for an Induction Motor Drive", *Hindawi Complexity*, Vol. 2019, p. 24, 2019.

[12] C. M. R. Oliveira1, M. L. Aguiar, J. R. B. A. Monteir, W. C. A. Pereira1, G. T. Paula, and T. E. P. Almeida, "Vector Control of Induction Motor Using an Integral Sliding Mode Controller with Anti-windup", *J Control Autom Electr Syst*, 2016.

[13] B. Aichi and K. Kendouci, "A Novel Switching Control for Induction Motors Using a Robust Hybrid Controller that Combines Sliding Mode with PI Anti-Windup", *Periodica Polytechnica Electrical Engineering and Computer Science*, Vol. 64, No. 4, pp. 392-405, 2020.

[14] H. Acikgoz, "Real-time adaptive speed control of vector-controlled induction motor drive based on online-trained Type-2 Fuzzy Neural Network Controller", *Int Trans Electr Energ Syst*, 2020.

[15] N. T. Pham and T. D. Le, "A Novel FOC Vector Control Structure Using RBF Tuning PI and SM for SPIM Drives", *International Journal of Intelligent Engineering and Systems*, Vol. 14, No. 3, pp. 429-440, 2021.

[16] Y. Shtessel, C. Edwards, L. Fridman, and A. Levant, "Sliding Mode Control and Observation", *Springer Science Business Media New York*, 2014.

[17] J. W. Finch and D. Giaouris, "Controlled AC electrical drives", *IEEE Trans. Ind. Electron*., Vol. 55, No. 2, pp. 481-491, 2008.

[18] M. E. Mahfoud, B. Bossoufi, N. E. Ouanjli, M. Said, and M. Taoussi, "Improved Direct Torque Control of Doubly Fed Induction Motor Using Space Vector Modulation", *International Journal of Intelligent Engineering and Systems*, Vol. 14, No. 3, pp. 177-188, 2021.